ARRIVAL DIRECTION OF AURORAL HISS EMISSIONS DETERMINED BY TRIPARTITE OBSERVATION

Takesi NAGATA, Takeo HIRASAWA

National Institute of Polar Research, 9–10, Kaga 1-chome, Itabashi-ku, Tokyo 173

and

Masanori NISHINO

Research Institute of Atmospherics, Nagoya University, Honohara, Toyokawa 442

Abstract: A new direction finding technique (abbreviated as DF) for auroral hiss emissions is introduced based on the measurement of time differences of arrival of waves between three spaced observing stations. Two unmanned observatories for VLF hiss were built at positions about 20 km south and east from Syowa Station (geomagnetic lat. −69.6°), Antarctica. The VLF signals observed at these two unmanned stations are sent in real time to Syowa Station over 2 GHz wide-band telemetry systems. The arrival time differences of VLF hiss signals between Syowa Station and each unmanned station are automatically determined by cross-correlating the wave forms of the received signals. The arrival directions of hiss emissions are determined by the tripartite observation method. The accuracy of the whole system is about 10° in incident and azimuthal angles. A comparison of the results obtained with those of ground-based auroral data has shown that the arrival directions of auroral hiss correspond well to the bright aurora areas at the ionosphere level and that they change rapidly in accordance with movements of the aurora.

1. Introduction

The direction finding technique (DF) of VLF emissions has been made in two different ways: (a) DF by means of directive antennas and (b) measurements of time differences of wave arrival at three spaced stations. ELLIS and CARTWRIGHT (1959) first observed the arrival direction of mid-latitude VLF emissions using the goniometer method. Though the goniometer DF method is useful for linearly polarized waves propagated horizontally, auroral VLF hiss emissions which are observed in the high-latitudes in close association with auroral displays, are propagated downwards with elliptical wave polarization. TANAKA *et al.* (1976) tried to measure the direction of arrival of auroral VLF hiss at Syowa Station, using a DF method based on the analysis of Lissajous figures of electric and magnetic fields displayed on cathode ray tubes. The measuring accuracy of this DF method was often decreased due to impulsive atmospherics, the peak intensity of which was

usually larger by about an order of 2 in magnitude over that of auroral VLF hiss. MAKITA (1979) observed the arrival direction of auroral VLF hiss at Syowa Station using the algebraic computation method developed by TSURUDA and HAYASHI (1975). The measuring accuracy of this DF depends sharply on the wave polarization as well as on the incident angle.

We have developed a DF for auroral VLF hiss based on the measurement of time differences of wave arrival, which is independent of the wave polarization as well as of the waveform. The arrival time differences among the signals received at the three spaced observing points are determined by computing the cross-correlation among the wide band signals received, so that the interference of impulsive atmospherics is reduced. The purpose of this paper is to describe the new DF system and to emphasize the validity of this DF system. A comparison of the results of direction of arrival of auroral hiss with the auroral data also is presented.

2. DF System

Fig. 1 shows the configuration of the three observing points and the block diagram of the DF system. The three observing points are composed of the main point (M) at Syowa Station on East Ongul Island, a satellite points (S_1) at 30 m above the sea level at Langhovde, and a second satellite point (S_2) on an ice slope of the Antarctic Continent at 430 m elevation above sea level. The distance between M and S_1 is 19.2 km, and that between M and S_2 is 18.2 km. The intersecting

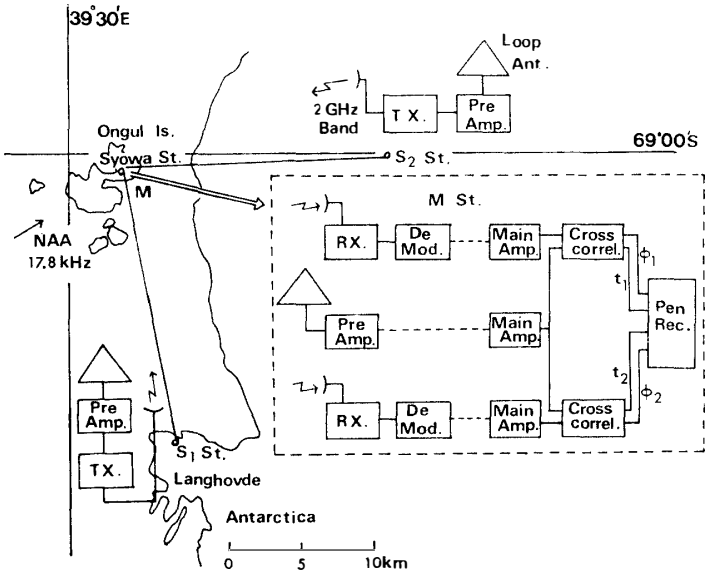

Fig. 1. DF system for auroral hiss based on the measurement of differences of time of arrival; configuration of the three observing points (M, S_1 and S_2) and the block diagram of the DF system.

angle between the two base lines (M–S_1 and M–S_2) is 80.0°. Auroral hiss signals received by a loop antenna at each satellite unmanned station (S_1 and S_2) are amplified by a wide band preamplifier (0.3–100 kHz) and transmitted by a 2 GHz wide-band telemeter from each satellite station to Syowa Station.

2.1. Determination of wave arrival time differences

As the spectrum intensity of auroral hiss shows a maximum in a frequency range of 5 to 20 kHz, the distances between Syowa Station (M) and each satellite observing station (S_1 and S_2) have been chosen to be about 20 km corresponding to the average wavelength in this frequency range. Fig. 2 presents a schematic diagram to show the method for determining the arrival time difference between hiss signals received at the two points (M and S_1). When the cross-correlation between the waveforms observed at S_1 and those observed at M becomes the maximum by taking the time-lag (τ) as $\tau=\tau_1$, the time-lag (τ_1) can be considered as the difference between the arrival time of the two waves.

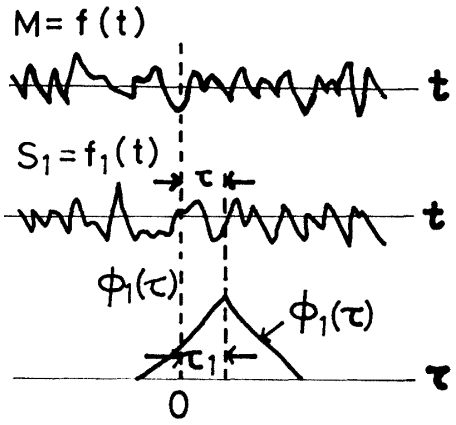

Fig. 2. Principle of the measurement of differences of time of arrival between the hiss signals at the two observing points (M and S_1) by cross-correlating the both waveforms.

Using the time differences τ_1 and τ_2 of arrival of the waves between M and S_1 and between M and S_2, the azimuthal angle (θ) and the incident angle (i) are found, on the assumption that the arriving hiss waves can be approximated by a plane wave model, by

$$\begin{cases} \tan\theta=\dfrac{\tau_2}{\tau_1}\dfrac{d_1}{d_2}\operatorname{cosec}\alpha-\cot\alpha \\ \sin i=c\operatorname{cosec}\alpha\sqrt{\left(\dfrac{\tau_1}{d_1}\right)^2+\left(\dfrac{\tau_2}{d_2}\right)^2-2\left(\dfrac{\tau_1}{d_1}\dfrac{\tau_2}{d_2}\right)\cos\alpha} \end{cases}$$

where τ_1 is the arrival time difference between M and S_1, τ_2 that between M and S_2, c the light velocity, and α is the intersecting angle between the two base lines (M–S_1 and M–S_2).

2.2. *Hiss receiver*

The loop antenna at each observatory is triangular with two turns and its dimensions are 8 m in height and 14 m base-length. These dimensions are the minimum possible for detecting the auroral hiss of flux density of 10^{-16} W/m^2 (Hz). The hiss signal induced in the loop antenna is amplified by a step-up transformer with a high turn ratio and low noise pre-amplifier, and is fed to a level amplifier which has an attenuator to adjust the signal intensity for the telemeter.

2.3. *Telemetry system*

The frequency spectrum of auroral hiss often extends beyond 100 kHz. A wide-band telemeter with a carrier frequency of about 2 GHz was employed to transmit and receive the wave signals of frequency bandwidth of 0.3–100 kHz. The transmitting and receiving antennas adopted were paraboloidal with diameter 1.2 m and gain 24.2 dB. The performance characteristics of the transmitter-receiver is shown in Table 1, and that of the overall telemetry system in Table 2.

Table 1. Characteristics of the transmitter-receiver (NEC TR-2G960).

1) Transmitter-receiver	
Transmission frequency	S_1–M, 1989 MHz
	S_2–M, 1859 MHz
Modulation	F M
Transmission frequency band	0.3–100 kHz
Frequency deviation	200 kHzrms
2) Transmitter	
Power	0.3 W
Frequency stability	$<\pm 8\times 10^{-5}$
3) Receiver	
Noise figure	7.5 dB
Intermediate frequency	70 MHz
Frequency stability	$<\pm 5\times 10^{-5}$
4) Power consumption	
Transmitter	$<$ 4 W
Receiver	$<$ 7 W

2.4. *Correlator*

Two delay times τ_1 and τ_2 are determined by the cross-correlation method using three digital memories (IWATSU DM305) and a data processor (IWATSU SM1330). The three hiss signals observed at the three spaced stations are fed to each digital memory, where the analogue signal is converted to digital and then stored. The digitalized data are transferred to the data processor by clock pulses

in the data processor. The program of cross-correlation calculates the differences of time of arrival (τ_1 and τ_2) and the cross-correlation coefficients ($\phi_1(\tau_1)$ and $\phi_2(\tau_2)$). These values are then averaged and converted to analogue, and recorded on a pen-recorder. The performance characteristics of the digital memory (DM305) is described in Table 3, and those of the data processor (SM330) in Table 4.

The delay times for the wave propagation through the telemeter system and

Table 2. Characteristics of transmission lines from the satellite points (S_1 & S_2) to the receiving point at Syowa Station.

1) TX output power	24.8 dBm	0.3 W
2) Propagation loss	−127.5 dB −124.5 dB	M–S_1 (18.9 km) M–S_2 (18.5 km)
3) Feeder loss	−2.0 dB −2.0 dB	TX, 8D2W, 5 m RX, 8D2W, 5 m
4) Antenna gain	24.2 dB 24.2 dB	TX, 1.2 mϕ, paraboloidal antenna RX, 1.2 mϕ, paraboloidal antenna
5) Line loss	−83.1 dB −80.1 dB	M–S_1, (2)+(3)(TX+RX)+(4)(TX+RX) M–S_2, (2)+(3)(TX+RX)+(4)(TX+RX)
6) RX receiving power	−58.3 dBm −55.3 dBm	M–S_1, (1)+(5) M–S_2, (1)+(5)
7) Receiver noise	−94.7 dBm	B=15 MHz, NF 7.5 dB
8) Carrier to noise ratio (C/N)	36.4 dB 39.4 dB	M–S_1, (6)−(7) M–S_2, (6)−(7)
9) Improvement factor of signal to noise ratio (S/N)	32.6 dB	FM improvement factor
10) S/N of the lines	69.0 dB 72.0 dB	M–S_1, (8)+(9) M–S_2, (8)+(9)

Table 3. Main characteristics of the digital memory (IWATSU DM 305).

Memory capacity	8 bits × 1024 words
Maximum conversion time of A-D converter	1 μs/word
Memory circuit	MOS STATIC RAM
Input voltage range	±0.1 V − ±50 V
Input frequency band	DC-250 kHz
Reading	Automatic repeat

Table 4. Main characteristics of the data processor (IWATSU SM 1330).

Memory circuit		Dynamic RAM, 16 bits × 12 kwords
Function		Cross-correlation
Data acquisition time		5 μs/word
Computation time,	256 words	About 0.45 s (Measured)
	512 words	0.83 s (〃)
	1024 words	1.60 s (〃)
Output	2 channels	Delay time (τ_1 and τ_2)
	2 channels	Coefficient of the cross-correlation (ϕ_1 and ϕ_2)
	Accuracy	3%
	Resolution	1/4096, 12 bits

the cable between M and S_1 and between M and S_2 respectively must be compensated. The necessary compensations are made with an accuracy of 1 μs by means of the pre-computation delay attached to the digital memory, where the compensation times are determined observationally by the azimuthal angle of the known direction of arrival for NAA (θ=295.0). The estimated delay time is 26.8 μs between M and S_1 and 29.8 μs between M and S_2, respectively.

2.5. *Measuring accuracy of direction of arrival*

The measuring accuracy of the DF depends mainly on the time resolution in computing the cross-correlation. The maximum sampling speed of the digital memory (DM305) is 1 μs, which corresponds to a resolution of 3° in measuring azimuthal and incident angles of noise-free signals. It is difficult, however, to

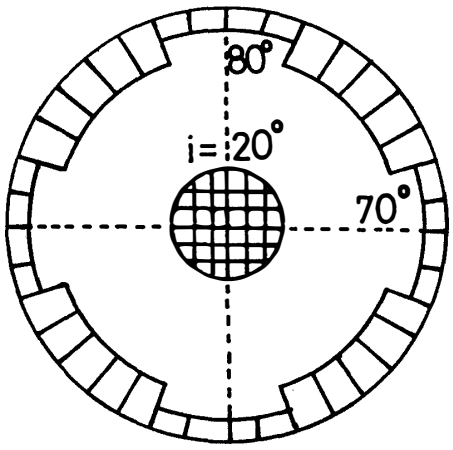

Fig. 3. Measuring accuracy of arrival directions for a time resolution of 3 μs. The azimuthal angle θ is measured anti-clockwise from the X-axis and the incident angle i is represented as the radial distance.

actually implement the time resolution of 1 μs for the total system of the DF because of noisy signals caused by the atmospherics as well as by other background radio noises. The actual measuring accuracy was statistically deduced from the distribution of the delay times of reception of NAA waves. Occurrence frequency distribution of these delay times was approximately a normal distribution, with a standard deviation of about 3 μs. The estimated accuracy of the direction of arrival calculated for a time resolution of 3 μs is shown schematically in Fig. 3. Between the central cross-hatched circle around the zenith (incident angle $\leq 20°$) and the hatched range near the horizon, the azimuthal and incident angles of the arrival directions can be determined in the accuracy of 10°. For small incident angles ($\leq 20°$), the estimate of the measurement accuracy of the DF based on the assumption of a plane wave is no longer valid and the measurement error of the DF for a spherical wave will have to be considered.

3. Observed Results

Fig. 4 shows an example of results of auroral hiss observations at Syowa Station on June 14, 1978; from the top to the bottom (a) the intensity of auroral hiss at 8 kHz recorded by means of a minimum level reading circuit (TANAKA, 1972), (b) the

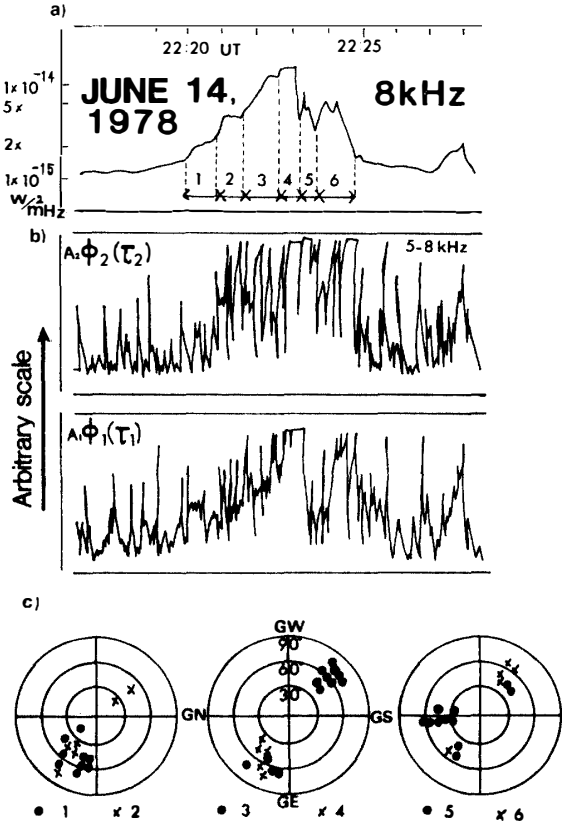

Fig. 4. Temporal evolution of observed results at 22h UT, June 14, 1978 at Syowa Station.
(a) Intensity of 8 kHz auroral hiss.
(b) Cross-correlation coefficients of $\phi_2(\tau_2)$ and $\phi_1(\tau_1)$ for received hiss signals at 5–8 kHz.
(c) Estimated azimuthal and incident angles of auroral hiss. The numbers from 1 to 6 represent 6 sub-events.

cross-correlation coefficients ($\phi_1(\tau_1)$ and $\phi_2(\tau_2)$) in the 5–8 kHz frequency band, and (c) the estimated azimuthal and incident angles of auroral hiss. When auroral hiss did not occur (22h17m–20m and 22h25m–28m), $\phi_1(\tau_1)$ (cross-correlation between M and S_1) and $\phi_1(\tau_2)$ (between M and S_2) show sharp spikes due to intense atmospherics, and in between fall to the zero level. When auroral hiss began to occur at about 22h20m, the minimum level envelope of the cross-correlation coefficients increases, almost parallel to the hiss activities. This characteristic of the present DF-system may prove its validity. Based on the delay time data during the hiss occurrences, the directions of arrival of the auroral hiss are determined and are shown at the bottom of Fig. 4.

As illustrated in panel (a) of Fig. 4, the hiss event with a duration of five minutes (from 22h20m to 25m) can be divided into six sub-events, according to the spike-type enhancements in hiss intensity variation, as shown in the figure. It is found from the results of panel (a) and panel (c) that the auroral hiss is propagated from localized regions moving with time and that the sub-events of auroral hiss show nearly one-to-one correspondence to certain localized sources. From the above results, the present new DF can follow rapid motions of sources of auroral hiss, whence a comparison of directions of the arrival of auroral hiss with observed auroral motions becomes possible leading to physical interpretations. The directions of arrival of auroral hiss are compared below with the all-sky photographs of aurora for three hiss events.

3.1. 22h UT, July 4, 1978 (Fig. 5)

A spike-type auroral hiss event occurred at 22h46m simultaneously with a sharp negative decrease of the geomagnetic *H* component. During the short period of the auroral hiss of about 2 minutes duration, there appeared 4 spike-type enhancements in the auroral hiss intensity (panel (a)). When the directions of arrival of these 4 sub-events auroral hiss are compared with the auroral behavior illustrated in all-sky photographs in panel (c), the following characteristics can be observed.

(1) The left hand all-sky auroral photograph (22h47m UT) of panel (c) shows that the folding form auroral arcs were extending above the geomagnetic northern (GN) horizon. The folding aurora was traveling from geomagnetic east (GE) to west (GW). Corresponding to these intense auroral arcs, the auroral hiss was first received at an incident angle of about 70° from GWNW direction, and then its azimuthal angle changed from GWNW to GNNE.

(2) The aurora which brightened near the northern horizon suddenly expanded towards the zenith at 22h48m. In association with the auroral motion, the auroral hiss arrived at an incident angle of about 50° from GN direction, and then its directions of arrival changed toward the GENE direction at an incident angle of about 60°. Subsequently the intensity of auroral hiss abruptly decreased simultaneously with the wide expansion of bright aurora around the zenith, due to the

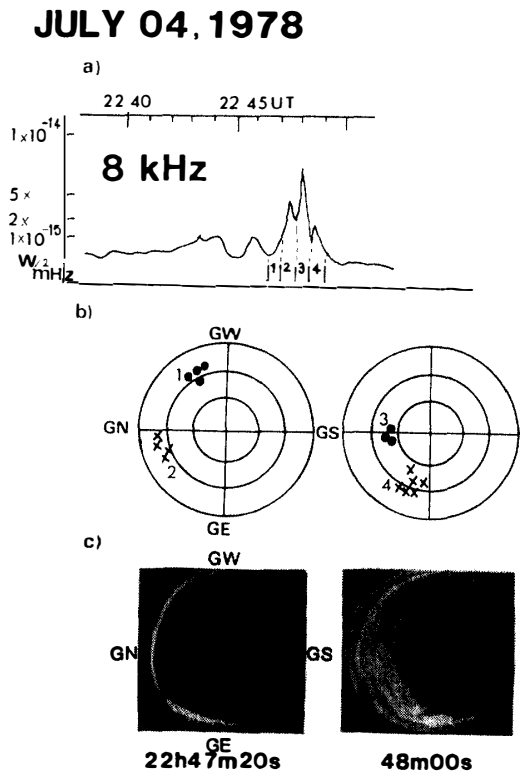

Fig. 5. Temporal evolution of observed results at 22h UT, July 4, 1978 at Syowa Station.
(a) Intensity of 8 kHz auroral hiss.
(b) Estimated azimuthal and incident angles of auroral hiss at 5–8 kHz.
(c) All-sky photographs of aurora.

heavy absorption of the hiss in the lower ionosphere ionized by precipitating auroral particles. The decay of the auroral hiss intensity corresponded to the maximum decrease of the geomagnetic H component.

3.2. 19h UT, June 26, 1978 (Fig. 6)

3 sub-events of auroral hiss each with a duration of about one minute occurred subsequently during the maximum decrease of a small negative geomagnetic bay. A comparison between arrival directions of these successive 3 sub-events of auroral hiss and the auroral motion shows the following relationships.

(1) The all-sky photograph of aurora at 19h00m00s shows ray-structured auroras observed in the GS and GSSE directions. At that time, the auroral hiss arrived from the corresponding regions of the ray-structured auroras; namely, at an incident angle of about 80° and from the GS direction and at about 50° from the GSSE direction.

(2) It is observed in the all-sky photographs at 19h00m00s and 02m00s that multi-band folding form auroras brightened near the GW horizon and then traveled rapidly from GW towards GE. Corresponding to the auroral behavior, the auroral hiss arrived from a localized region around the GW horizon. In the all-sky photograph at 19h02m00s, another auroral movement was observable in the GS. It began to move from GS to GW in a meandering form with increasing activity.

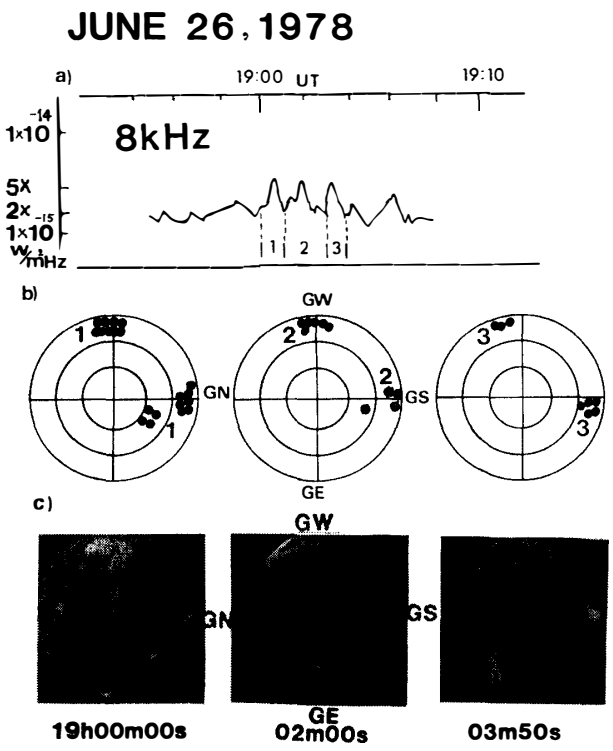

Fig. 6. Temporal evolution of observed results at 19h UT, June 26, 1978 at Syowa Station.
(a) Intensity of 8 kHz auroral hiss.
(b) Estimated azimuthal and incident angles of auroral hiss at 5–8 kHz.
(c) All-sky photographs of aurora.

The auroral hiss came from the direction of the GS horizon in associated with this auroral movement.

(3) As shown in the photograph at 19h03m50s, the luminosity of the two auroras along the GW and GS horizons remained considerably strong, though their structures became obscure. The auroral hiss arrived from these localized regions in the GW and GS.

3.3. 20–21h UT, June 26, 1978 (Fig. 7)

Relatively intense auroral hiss, about 10 minutes in duration, occurred during a gradually decreasing phase of a large negative geomagnetic bay, as shown in panel (a) of Fig. 7. During the hiss event, the auroral activity is variable in motion and in structure. In order to compare the arrival directions with all-sky photographs of aurora, the hiss event is divided into 9 sub-events with reference to the spike-type variations of its intensity.

(1) Various types of aurora were observed in the all-sky photograph at 20h57m00s; multiple bands of auroras in GW direction, dispersive rays in GN and a homogeneous band in GS horizon. Auroral hiss emissions came from the two regions of active multi-bands and rayed auroras in GW and GN directions, but not from the region of the occurrence of the homogeneous band.

(2) Intense auroral hiss emissions (No. 2 sub-event) arrived from the region

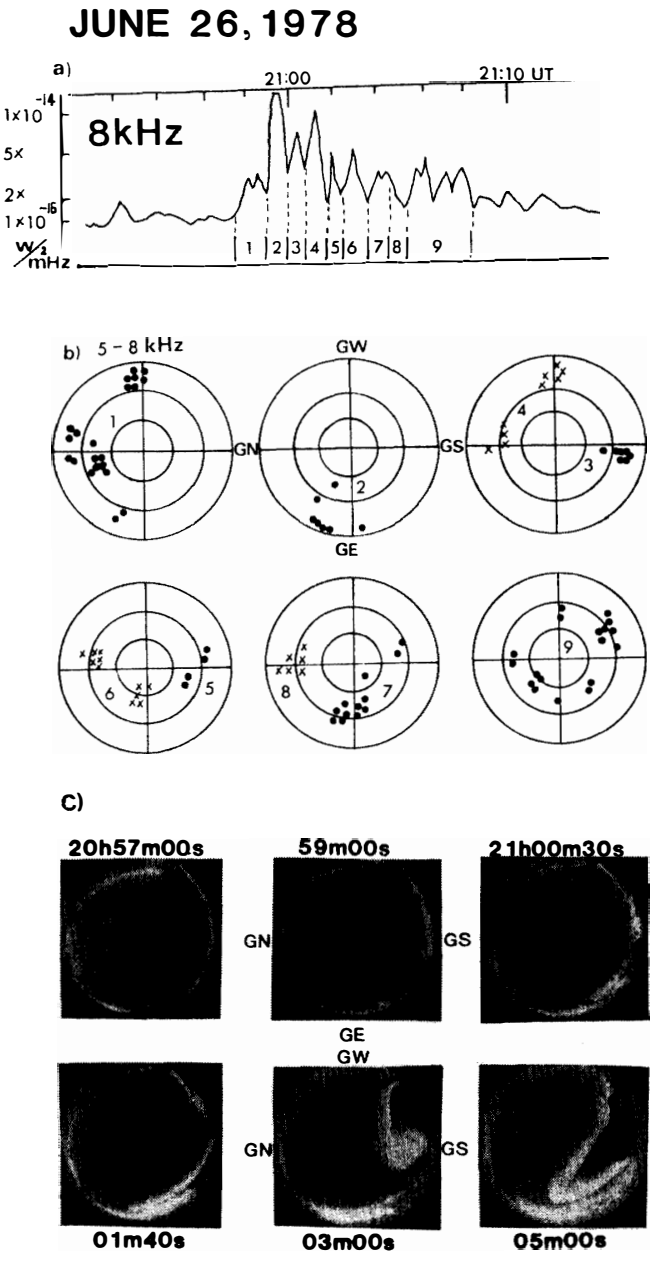

Fig. 7. Temporal evolution of observed results at 20–21h UT, June 26, 1978 at Syowa Station.
(*a*) *Intensity of 8 kHz auroral hiss.*
(*b*) *Estimated azimuthal and incident angles of auroral hiss at 5–8 kHz.*
(*c*) *All-sky photographs of aurora.*

near the horizon of GE direction, where two or three movements of folding auroras were observed in the all-sky photograph at 20h59m00s.

(3) As is clearly seen in the all-sky photographs at 21h00m30s, 01m40s, 03m00s and 05m00s, a bright auroral band became active above the GS horizon at 21h00m30s, and then it began to fold while rapidly moving eastwards. The auroral movement lasted from 21h00m30s to 05m00s and the auroral band extended towards the zenith. Corresponding to this auroral display, the direction of arrival of auroral hiss emis-

sions (No. 3, 5, 7 and 9 sub-events) changed rapidly in accordance with the motion of the bright aurora.

(4) During the period from 21h00m30s to 05m00s, diffuse rayed auroras also became active in the northern part of the sky. Corresponding to these auroral activities, auroral hiss emissions were received sccessively from the directions of GW and GN (No. 4, 6 and 8 sub-events).

4. Summary

Based on the above three observed results, it may be concluded that the auroral hiss emissions with a duration of about 10 minutes or so can be divided into several sub-events with an average duration of about 1 minute with reference to the spike-type enhancements in their intensity records. The direction of arrival of each sub-event auroral hiss emission corresponds well to a localized active region of simultaneous aurora. It is also found that the arrival directions of auroral VLF hiss do not always coincide with the whole region of brightening aurora, but with a special part of the aurora which rapidly changes in luminosity and motion.

OGUTI (1976) has analyzed real-time auroral records on a video tape obtained with a highly sensitive TV camera at Syowa, and simultaneous records of VLF waves on the sound track of the same video tape. He has identified the hiss emitting from aurora by cross-correlation analysis between the temporal variations in luminosity of auroral structures and the temporal variations of hiss intensities; the auroral hiss is associated with specific characteristics of aurora, such as rapid brightening and rapid motions, and it is not associated with quiet auroras which have no remarkable motions nor changes in luminosity.

OGUTI *et al.* (1979) have shown from results of simultaneous observations of auroral hiss and aurora at Churchill, Canada with an algebraic DF system (TSURUDA and HAYASHI, 1975) and an all-sky camera, that the auroral hiss emerges from a newly born branch of the auroral arc. The three observational results mentioned above have also confirmed the association of auroral hiss with active aurora, with a higher accuracy.

5. Conclusion

A new direction finding system based on the measurement of arrival time differences among three spaced stations has been developed for the study of auroral VLF hiss. From the new DF data of auroral hiss compared to all-sky photographs of aurora, it has been clearly found that the arrival direction of auroral VLF hiss coincides with a local region of active aurora. Further analyses of the data will provide valuable information for discussing the generation and propagation mechanisms of auroral VLF hiss. In order to improve the accuracy and reliability of the present DF system, the better design will be required, taking into consideration of

the relation between the data-processing time and space and time resolution of the movement of the direction of arrival of auroral hiss. An important observational problem is that the instrument at the unmanned station must operate stably under the severe meteorological circumstances in Antarctica.

Acknowledgment

The authors acknowledge Prof. A. IWAI and Dr. Y. TANAKA of Research Institute of Atmospherics, Nagoya University for their valuable discussions. The authors also wish to express their gratitude for the kind cooperation given by the wintering members of the 19th Japanese Antarctic Research Expedition, for the construction and maintenance of the DF system in Antarctica.

References

ELLIS, G. R. A. and CARTWRIGHT, C. A. (1959): Directional observations of noise from the outer atmosphere. Nature, **184**, 1307–1308.

MAKITA, K. (1979): Auroral hiss observations both on the ground and the satellite-Estimations of the generation region and the propagation path. Magnetospheric Study 1979: Proceeding of the International Workshop on Selected Topics of Magnetospheric Physics. Tokyo, Japanese IMS Committee, 277–281.

OGUTI, T. (1976): Hiss emitting auroral activity. J. Atmos. Terr. Phys., **37**, 761–768.

OGUTI, T., HAYASHI, K., KOKUBUN, S., TSURUDA, T., WATANABE, T. and HORITA, R. E. (1979): Relation between auroral precipitation and VLF waves. Magnetospheric Study 1979: Proceeding of the International Workshop on Selected Topics of Magnetospheric Physics. Tokyo, Japanese IMS Committee, 253–257.

TANAKA, Y., HAYAKAWA, M. and NISHINO, M. (1976): Study of auroral VLF hiss observed at Syowa Station, Antarctica. Mem. Natl Inst. Polar Res., Ser. A (Aeronomy), **13**, 58p.

TSURUDA, K. and HAYASHI, K. (1975): Direction finding technique for elliptically polarized VLF electromagnetic waves and its application to the low-latitudinal whistlers. J. Atmos. Terr. Phys., **37**, 1193–1202.

(Received May 1, 1980)